

**Evaluating the Transferability of a Real-Time Global Traffic Data Source  
for Urban NO<sub>2</sub> Regression Models**

Author: Austin Singleton (AUC)

[austinasing@gmail.com](mailto:austinasing@gmail.com)

Supervisor: Dr. Eduardo Simao da Graca Dias (VU)  
[e.simaodagracadias@vu.nl](mailto:e.simaodagracadias@vu.nl)

Reader: Dr. Eric Koomen  
[e.koomen@vu.nl](mailto:e.koomen@vu.nl)

Tutor: Dr. Anco Lankreijer  
[a.c.lankreijer@auc.nl](mailto:a.c.lankreijer@auc.nl)

Date of submission: June 7 2023

Science Major

Word count: 6100

## Abstract

As air pollution continues to be a major health risk in many cities around the world, the lack of options for low-cost air quality monitoring has left many cities in lower middle income countries (LMICs) to be without knowledge on the concentration and variation of deadly air pollutants. In recent years, the web-application Google Maps Traffic (GMT) has been proposed as a low-cost high resolution source of traffic data to inform air pollution models. Due to its global reach, GMT may especially be an ideal pollution predictor variable for transferable air pollution models, but this potential advantage has yet to be explored. This research aims to investigate how the inclusion of Google Maps traffic as a predicting variable impacts the accuracy of different transferred models. This is achieved by developing a series of Land Use Regression (LUR) models for the five largest cities in the Netherlands. Then the impact of the inclusion of GMT is evaluated with four tests on different kinds of transferable models. While inter-urban generalized models ranged from  $r^2 = 0.39-0.64$ , models tested and trained in different cities had much lower accuracy with many of them having zero predictive capability. The lack of overall model success was coupled with minimal from GMT including. While an overall advantage over historical traffic values can be identified, more research is required to determine the full potential of GMT for transferable air pollution models.

## Table of Contents:

<b>Abstract .....</b>	<b>1</b>
<b>Introduction .....</b>	<b>3</b>
<b>Study Area .....</b>	<b>6</b>
<b>Research Context .....</b>	<b>9</b>
<b>Methodology .....</b>	<b>12</b>
<b>Results .....</b>	<b>21</b>
<b>Discussion .....</b>	<b>27</b>
<b>Conclusion .....</b>	<b>29</b>
<b>Works Cited .....</b>	<b>30</b>
<b>Appendix .....</b>	<b>39</b>

### Key Phrases:

- Transferability
- Google Maps Traffic
- Urban Air Pollution
- Artificial Neural Networks
- Land Use Regression

### Abbreviations:

ANN = Artificial Neural Network  
 GMT = Google Maps Traffic  
 LMIC = Lower- Middle Income Country  
 LUR = Land Use Regression  
 MLP = Multi-Layer Perceptron  
 MSE = Mean Squared Error  
 $r^2$  = Coefficient of Determination  
 RI = Relative Importance

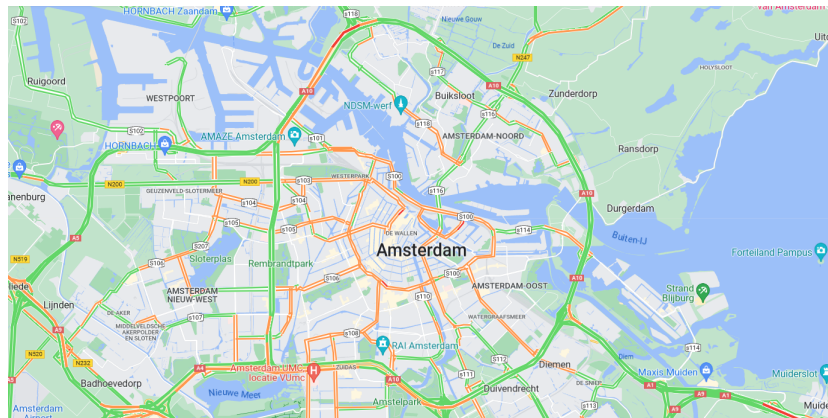
## Introduction

As urbanization and vehicle use continues to rise in the 21st century, air pollution is becoming a leading global environmental risk. This has led to air pollution being associated with 6.7 million premature deaths annually (Health Effects Institute, 2020). The proliferation of vehicles has caused serious urban and regional air pollution amongst cities in lower- and middle income countries (LMICs). As of 2018, these countries account for 90% of the global urbanization process (Zhang et al., 2022). This is causing cities in LMICs to be at more risk as 98% of cities in low- and medium-income countries are not meeting WHO air quality guidelines (WHO, 2016). A contributing factor to this is the lack of information and monitoring that leave regions in Africa, Eastern Europe, and South Asia to have little or no recorded data about their air quality (Karagulian et al., 2015). Monitoring is an integral part of air pollution management, but lack of detailed information on air pollutants is widespread in many LMICs due to the high cost of installing and maintaining on-ground measurement systems (Martin et al., 2019). For many air pollution models, traffic-related measurements are a key variable to predicting pollutant variation (Dijkema et al., 2011). However, high resolution traffic data to analyze city-size variation requires an increasing high density of costly traffic measurement tools. This has caused conventional monitoring systems to be very economical with many high accuracy models concentrated and localized in cities of high income countries (Idrees & Zheng, 2020).

Current solutions to make air quality monitoring more accessible to LMICs include: low cost ambient sensors, portable monitoring, satellite remote sensing, and internet of things(IoT)(Idrees & Zheng, 2020). This study aims to investigate a recent exploration in low-cost traffic monitoring: Google Maps Traffic (GMT).

In 2007, Google launched arterial traffic information on their web mapping and navigation platform: Google Maps. This allowed users to see maps of traffic congestion to avoid driving through high traffic areas (Google Blog, 2009a). These maps are crowd-sourced by devices in vehicles connected to Google Maps that are constantly informing a Google model with speed and location information (Google Blog, 2009b). This kind of data collection is known as Floating Car Data (FCD), and is becoming more widely used in traffic analysis as more geo-data becomes accessible. Google Maps is the most widely used navigation app and thus, with reportedly up to a billion monthly users worldwide, collects and supplies high-resolution real-time FCD for free to most people around the world (Russell, 2019; Google, 2023b). In recent years, Google Maps has been recognized as a global traffic measurement alternative for: queue-length estimation, traffic reduction effectiveness, and as a predictor of air pollution (Sornsoongnern et al., 2023; Hanna et al., 2017; Rybarczyk & Zalakeviciute, 2017).

Figure 1: Screenshot of the Google Maps Traffic Layer in Amsterdam



Its global reach and openly accessible data gives GMT high potential as a low-cost traffic measurement tool. Its particular benefit for LMICs has additionally been expressed in studies in Ecuador and Morocco (Rezzouqi et al., 2018; Rybarczyk & Zalakeviciute, 2017). Its geographic spread also makes Google Maps Traffic especially suitable for transferability-focused models as

the traffic data is continuous around the world. Transferability is defined as, "the extent to which a model developed for one place can be applied to other areas"(Ma et al., 2022). More focus in recent years has been on the development of these transferable models so that more areas can have access to pollution monitoring even without routine air quality collection (Ma et al., 2022). Most transferable models are Land Use Regression models (LUR). LUR modeling uses land use, traffic characteristics, meteorology, and many other variables to explain the spatial variation of measured air pollution concentrations using statistical regression (Patton et al., 2015). This wide range of potential data sources, many of which don't require on-ground dedicated measurement, make LURs particularly useful for transferability.

While Google Maps Traffic has been applied for air pollution prediction in a few cases, its usage in air pollution is not widespread, and no research has thus far evaluated its use for transferability. Location specific models are known to perform very poorly when directly transferred to other areas and the chosen predictor variables have been identified as key determinants of this performance(Hoek et al., 2008). The usefulness of predictor variables can change drastically when transferred to other areas. While Google Maps' spatial unboundedness seems optimal for transferable models, this relationship has not been directly studied. Therefore, this research aims to novelly evaluate Google Maps traffic for its use in transferable air pollution models.

To do this, a series of Artificial Neural Network (ANN) LUR models are developed for major cities in the Netherlands to predict for Nitrogen Dioxide ( $\text{NO}_2$ ) variation.  $\text{NO}_2$  is chosen as  $\text{NO}_2$  models are found to be useful for transferability and most of its concentration in cities comes from traffic (Wang et al., 2014). Multiple sources of data were collected so that the LUR

models have a range of potential NO<sub>2</sub> predictor values. These included multiple meteorological values, surrounding land-use, and local fuel and vehicle types along with Google Traffic Data. These predictors are processed in their raw state, selected, and then trained in an optimized (ANN) alongside the NO<sub>2</sub> data.

The capabilities of Google Maps Traffic for transferability are evaluated by testing the impact that its inclusion has upon the predictive accuracy of the transferred model. Models for four different tests of transferability are created: A inter-urban Leave-One-Out-Cross-Validation (LOOCV), an intra-urban Hold-out Validation (HV), an intra-urban LOOCV, and a HV for the general model. LOOCV refers to removing one of the samples from a set (i.e. a station in a city or a city in a region) for training, and testing how accurate the rest of the set is for predicting each sample (Ma et al., 2022). HV instead refers to evaluation of a model to an independent site from its development (Ma et al., 2022). For each test, a baseline model with optimal input variables and model architecture is found and evaluated. Then, the accuracy is compared between the same model but with GMT as an additional predictor variable. A third model utilizing 2022 average traffic volume per hour per day is also compared to evaluate GMT against another method of low-cost traffic data. Utilizing different tests of transferability allows for further insight on which model situations GMT might be most suited for.

## **Study Area: The Netherlands**

The study area of this research consists of six cities in the Netherlands (in descending size): Amsterdam, Rotterdam, Den Haag, Utrecht, Eindhoven, Heerlen. The Netherlands is a small, low elevation, flat country. Therefore, the most populous cities are very close to each other and the climate and topography is relatively similar between them (World Bank Group,

2021). These aspects make the Netherlands well suited for transferability, which has been seen in multiple studies of transferable LUR models since 2006(Wang et al., 2014). In 2021, the Netherlands complied with the EU N02 limits along traffic roads for the first time since they were put into place in 2009 (RIVM, 2021). The country has been steadily decreasing the national average of urban NO<sub>2</sub> measurements from 35.7 µg/m<sup>3</sup> in 2011 to 21.7 µg/m<sup>3</sup> in 2020, where there was 0% population exposed to concentrations above NO<sub>2</sub> standards (European Environment Agency, 2021). Amsterdam, Rotterdam, Den Haag (The Hague), Utrecht and Eindhoven are the five largest cities in the country and have the highest density of monitoring (at least three NO<sub>2</sub> stations per city was decided as the minimum requirement). Heerlen is chosen as the most topographically different area to test the limits of transferability.

Figure 2: Map of 6 City Study Areas in the Netherlands

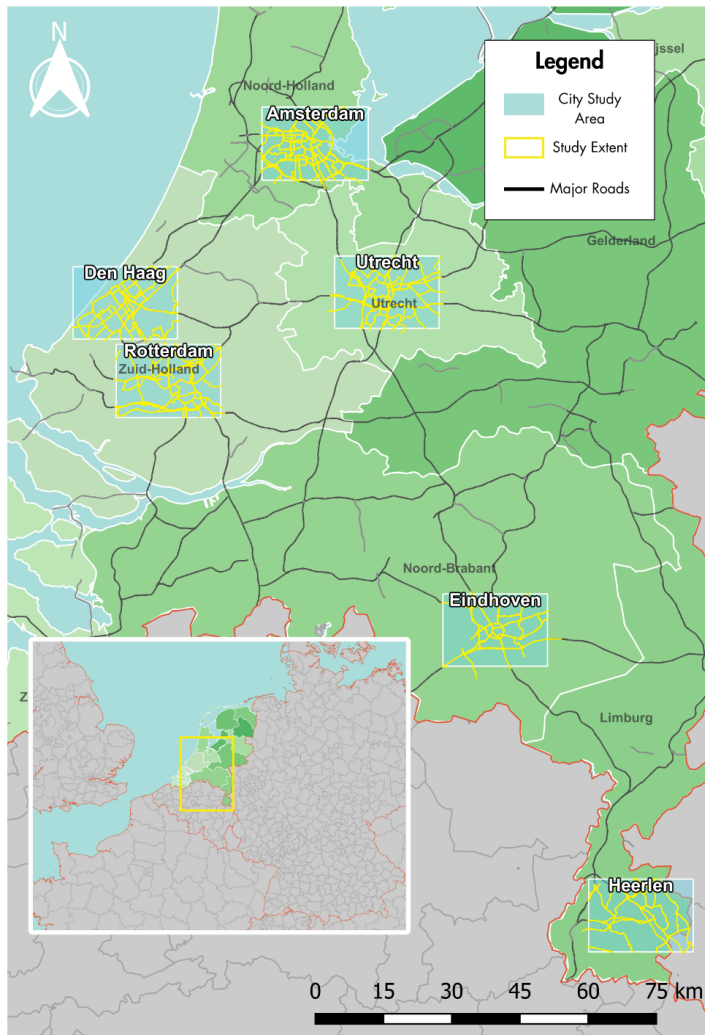
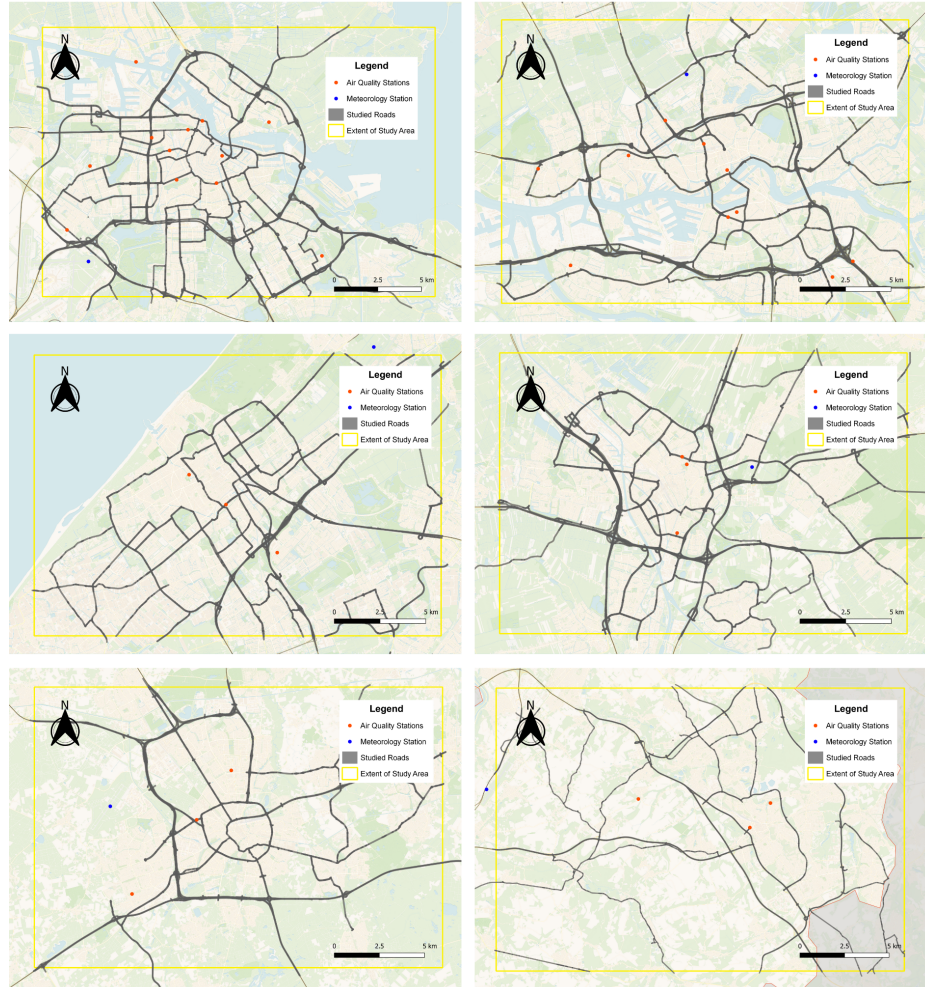


Figure 3: Maps of Individual Study Areas (Amsterdam, Rotterdam, Den Haag, Utrecht, Eindhoven, Heerlen)



The Netherlands provides many advantages that supplement developing and assessing air pollution models. Most importantly is the network of hourly air quality supplied by a coalition of monitoring networks that is openly accessible via the Luchtmeetnet website and API (Luchtmeetnet, 2020). This along with other openly-available data sources collected and supplied mostly by organizations of the Dutch government, is what makes this research possible to be free and only utilizing openly accessible data. So while this study area does not directly address the motivation of the research to explore methods of low-cost monitoring in LMICs, it is still useful for developing and testing the potential for low-cost methods.

## Research Context

This research is situated along multiple academic contexts of air pollution prediction, the field is first summarized, then the details of important related research are reviewed.

### Air Pollution Modelling

Urban-scaled air pollution modelling began in the early 1970's with models depending on mathematical approximations of chemical and physical processes to predict long-range transport dispersion for point sources (Daly, 2007). As the leading environmental concern in Europe at the time was for acid rain, these models were made specifically to address point sources like factories. As risk due to vehicle pollution has become a more important aspect of urban air pollution models, other methodologies have been similarly developed to address them. Today, urban air pollution models exist in two categories. The first type of model simulates dispersal and transport mechanisms of compounds from detailed data on the emission sources (Alimisis et al., 2018). These models, such as the popular Operational Street Pollution Model (OSPM), are very common for specific city locations and are optimized for accuracy in their area (Tang & Wang, 2007). The second approach uses statistical models to relate large amounts of data from potential predicting variables and measurements of air quality. In recent years these statistical models increasingly utilize machine learning methodologies such as Random Forests, Support Vehicle Machines, and Artificial Neural Networks to optimize model prediction (Chen et al., 2019).

### Transferable LURs

One of the many kinds of air pollution models that uses a statistical approach is a Land Use Regression (LUR). LURs are empirical regression models that combine air pollution

concentrations monitored in a limited number of locations with a number of potential predictor variables collected in a geographic information system(GIS)(Chen et al., 2019). As mentioned in the introduction, this type of methodology is most widely used in the development of transferable models. The first cited transferable LUR was a part of the SAVIAH study to apply an annual NO<sub>2</sub> model in Huddersfield, UK to four other UK cities (Patton et al., 2015; Hoek et al., 2008). This study used independent variables of road traffic, volume, land-use, and altitude and introduced a “regression-mapping” method of predicting NO<sub>2</sub> (Briggs et al., 2000). Regression-mapping is a more accurate name as land use is onlt one of multiple predictor variables in this methodology, but most researchers currently refer to it as land use regression (LUR)(Hoek et al., 2008). Models of this type have expanded over the years, in data sources and regression methods. In the Netherlands, NO<sub>2</sub> LURs have been utilized multiple times for health risk assessments, and it is a widely studied area of research (Beelen et al., 2007; Brauer et al., 2003).

The most successful study on transferability has been by the European Study of Cohorts for Air Pollution Effects (ESCAPE) studies, where 23 study areas in major cities and regions informed regional and European models. The study contained around 500 NO<sub>2</sub> sites around Europe, and evaluated the average of transferred models to have a r<sup>2</sup> of 0.59 (Wang et al., 2014). Most transferability is tested between cities as in the ESCAPE study or the 2011 study by Allen et al, on the transferability between major cities in Cananda (Allen et al. (2011). However, a few other studies have investigated inter-urban transferability by testing neighborhood-scale models to other neighborhoods or testing general city models on individual station generalizability (Patton et al, 2015; Ma et al., 2022).

### Artificial Neural Networks (ANN):

ANNs are mathematical models constructed of many interconnected nodes that are analogous to the structure of neurons in a brain (Alimisis et al., 2018). They are constructed of “neurons” or processing units that receive, process, and output numbers. This study uses a Multi-Layer Perceptron (MLP) Feed-Forward Neural Network (FFNN), which is one of the simplest yet widely used architectures. It is constructed by an input layer of neurons, the hidden layer(s) and an output neuron that are all connected to every other neuron in the layer next to it. In the context of this study, there are around 10 input neurons and one output neuron: the measured value of NO<sub>2</sub>. For every training set collected, the values of input neurons get passed on to the next layer through the output equation seen in figure 3. The model improves by changing the value of the weights of each connection ( $w_k$ ) and thresholds ( $\theta$ ) of each node so that the output node gets closer and closer to its real value (Yegnanarayana, 2009). The process of “learning” or optimizing which weights to change and how much is determined by a backpropagation algorithm which makes decisions based on the mean square error of the prediction.

Figure 4: Neural Network Activation Function

$$y = f \left( \sum_{i=1}^M x_i w_{ki} - \theta \right)$$

ANNs have been in widespread use in air pollution prediction in recent years, and have been successful in short- and long- term forecasting (Cabaneros, 2019). While there are many

types of ANNs, this research is only concerned with MLPs and does not investigate other machine learning methodologies in-depth.

### Google Maps Traffic Data

The first published use of Google Maps Traffic data for air pollution prediction was a 2017 study in Quito, Ecuador (Rybarczyk & Zalakeviciute, 2017). Since then, other published research has occurred in New York City, USA, California, USA, and Bangkok, Thailand. (Hilpert et al., 2019; Moon et al., 2022; Naiudomthum et al., 2022). The data source is utilized in two distinct ways. The first method involves high resolution screenshoting of the data to be processed into a raster (Zalakeviciute et al., 2020; Hilpert et al., 2019). The other methodology uses the Google API to create multiple routes between select areas and record the total delayed time per route (Naiudomthum et al., 2022; Moon et al., 2022). Hilpert et el., uses radar measurement to calibrate Google Maps traffic to levels of traffic flow, but all other methodologies use the data directly. The majority of this research has occurred in the past five years and all studies report success and high potential for future use of GMT. Each methodology has distinctly different goals and ranges of study of study area, but none investigate the transferability.

## **Methodology**

### Real Time Data Collection:

Traffic intensity, meteorology, and NO<sub>2</sub> data are collected via real-time hourly by a Python program running on a laptop. The program was set up from March 29 to May 29th to collect from these data sources hourly from 6am to 7pm. This short period helps reduce the effect

from seasonality, which can greatly impact NO<sub>2</sub> prediction (Eskes et al., 2008). While real time data collection is subject to more data gaps and unvalidated measurements, it is the only option for collecting GMT as Google does not archive the data publicly. Additionally, verified NO<sub>2</sub> values are released on the RIVM data portal up to a month after the collection period, which is not enough time for this study.

**Google Maps Traffic:** The traffic collection program works by opening a Google Maps url in an automated chrome browser with Selenium Webdriver (Selenium, 2023). The url of every Google Maps site includes the coordinate and zoom parameters of the map, so the program is able to open the same location and size of the map every time. Once the page is loaded, a screenshot is taken and the image RGB data for each pixel is saved to a csv for processing. This method of web scraping comes with its own difficulties and terms of service gray areas, so other applications of GMT have utilized the paid Google Maps API to collect traffic intensity data (Naiudomthum et al., 2022). However, the web scraping method was chosen due to its easier processing of spatial traffic information and so that the model could be done at no cost.

**Meteorology:** Hourly averaged meteorological measurements are collected via the KNMI API organized by the Royal Dutch Meteorological Institute. The closest stations to the study areas are found and their values are collected every hour. Models use a range of different predictors, but the most common variables are temperature, relative humidity, and wind measurements (Cabaneros et al., 2019). The maximum number of potential variables would be ideally gathered, but there were many large gaps in the data which caused variables such as solar radiation and precipitation values to be unusable. The collected meteorological values are temperature, wind speed, wind direction, relative humidity, and air pressure.

**NO<sub>2</sub>:** NO<sub>2</sub> is collected by the program via the Luchtmeetnet API(Luchtmeetnet, 2022). Luchtmeetnet is supplied by a collection of different organizations with multiple measurement stations alongside roads and in cities(Luchtmeetnet, 2020). The API is easily customizable and provides hourly data for 12 stations in Amsterdam, 10 in Rotterdam, and 3 in Den Haag, Utrecht, Eindhoven, and Heerlen. Because of its widespread and ease of use, other NO<sub>2</sub> collection methods were not considered.

Other Data Collection:

**Amount of Vehicles Per Fuel Type:** A table of the distribution of passenger cars based on the location of the end user from January 1st, 2020, to January 1st, 2021 collected by the Central Bureau of Statistics (CBS 2022a). This table collects total number of personal vehicles per province, and the separation by electric, plug-in hybrids, and over fuel types. This is used as a data source as some cities may have different concentrations of electric and non-electric vehicles, which would impact intra-urban transferability.

**Amount of Vehicles per Vehicle Type:** A table of the distribution of different classifications of vehicles based on the postal code they are registered in is collected by the Central Bureau of Statistics (CBS 2022b). This data provides the total road vehicles per city and its separation by commercial vehicles (buses, vans, tractors), trailers and semi-trailers, motorcycles, mopeds, and others.

**Land Use Data:** This study utilizes the 2018 Corine Land Cover Data (Copernicus, 2018) . This is a Europe-wide raster with 44 classes at 100m resolution created by the European Environmental Agency (Copernicus, 2018). This particular land-use set was chosen due to existing research on weighting the land-use classifications for optimal NO<sub>2</sub> prediction in a study in neighboring Belgium that could be expected to have accurate results(Janssen et al., 2008).

**Temporal Alternative to Traffic:** As discussed in the introduction, the central goal of this research is to evaluate the utility of Google Maps. A part of the evaluation is done by comparing how well the models that utilize Google Maps are to alternatives. The alternative used in this study is the average amount of traffic per hour for each day in each city. This model uses data from TomTom, another floating car data (FCD) traffic software application that publishes high resolution hourly traffic averages for cities in the Netherlands(TomTom, 2023). As seen in figure 5, the unit of this dataset is average travel time in the city per 10 km. Using this alternative allows Google Maps to be compared with another free traffic estimation method (though much less detailed and only available in select countries).

Figure 5: TomTom Average Travel Time  
Per 10km in Amsterdam (2022)

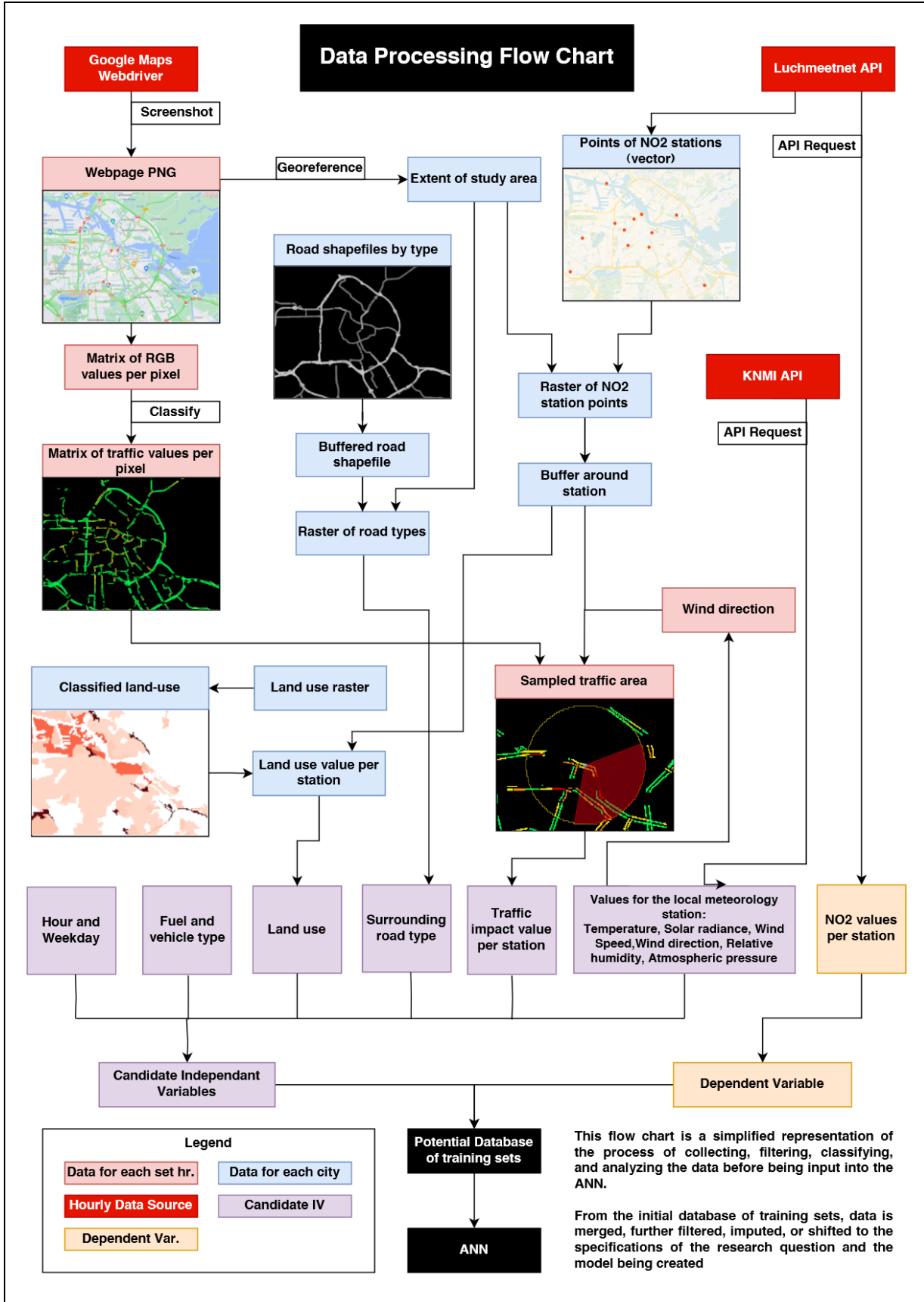
	Sun	Mon	Tue	Wed	Thu	Fri	Sat
12:00 AM	12 min 50 s	11 min 20 s	11 min 30 s	12 min	12 min	12 min 30 s	13 min 10 s
	12 min 40 s	11 min 20 s	11 min 20 s	11 min 50 s	12 min	12 min 30 s	13 min
02:00 AM	12 min 50 s	11 min 30 s	11 min 10 s	11 min 40 s	11 min 50 s	12 min 20 s	13 min 10 s
	12 min 50 s	10 min 50 s	10 min 30 s	11 min	11 min 10 s	12 min	13 min
04:00 AM	12 min 10 s	9 min 50 s	9 min 30 s	10 min	10 min	10 min 50 s	12 min 20 s
	11 min 30 s	8 min 50 s	8 min 40 s	8 min 50 s	8 min 50 s	9 min 20 s	11 min 20 s
06:00 AM	10 min 10 s	8 min 50 s	8 min 50 s	8 min 50 s	8 min 50 s	9 min	10 min
	9 min 50 s	10 min 10 s	10 min 20 s	10 min 10 s	10 min 10 s	10 min	9 min 40 s
08:00 AM	10 min	13 min 20 s	14 min 10 s	13 min	13 min 50 s	12 min	10 min 10 s
	10 min 20 s	12 min 50 s	13 min 50 s	12 min 50 s	13 min 40 s	12 min 20 s	10 min 50 s
10:00 AM	10 min 50 s	12 min 10 s	12 min 50 s	12 min 30 s	12 min 40 s	12 min 30 s	11 min 30 s
	11 min 10 s	12 min 20 s	12 min 50 s	12 min			
12:00 PM	11 min 50 s	12 min 40 s	12 min 50 s	13 min	13 min	13 min 10 s	12 min 20 s
	12 min 20 s	12 min 40 s	12 min 50 s	13 min	13 min	13 min 10 s	12 min 40 s
02:00 PM	12 min 30 s	12 min 50 s	13 min	13 min 10 s	13 min 10 s	13 min 40 s	12 min 50 s
	12 min 40 s	13 min 20 s	13 min 40 s	13 min 50 s	14 min 10 s	14 min 40 s	13 min
04:00 PM	12 min 40 s	13 min 10 s	14 min	14 min 10 s	14 min 50 s	14 min 40 s	12 min 50 s
	12 min 30 s	14 min 20 s	16 min 20 s	15 min 20 s	16 min 30 s	14 min 50 s	13 min
06:00 PM	12 min 10 s	13 min 30 s	15 min 20 s	14 min 30 s	15 min 50 s	14 min	12 min 50 s
	11 min 40 s	12 min 20 s	12 min 50 s	12 min 50 s	13 min 10 s	13 min	12 min 40 s
08:00 PM	11 min 20 s	11 min 50 s	12 min 10 s	12 min 10 s	12 min 20 s	12 min 40 s	12 min 20 s
	11 min 10 s	11 min 40 s	11 min 40 s	12 min	12 min	12 min 30 s	12 min 10 s
10:00 PM	11 min 10 s	11 min 30 s	11 min 40 s	11 min 50 s	12 min	12 min 40 s	12 min 20 s
	11 min 10 s	11 min 20 s	11 min 50 s	11 min 50 s	12 min 20 s	12 min 50 s	12 min 30 s

Additional details like data type, resolution, and overall quality for each data source can be found in the data table in Appendix A.

### Data Processing:

These sources of data come in dramatically different forms, but must be processed so that each predictor variable is represented by a single value for each training set. This process is summarized in figure 5, with additional details for each variable found after.

Figure 6: Data Processing Flow Chart



**Traffic:** To process the traffic screenshot, the program extracted only pixels of the image that contained relevant traffic data. The four traffic values from green to dark red are linearly normalized from 0 to 1. There is still no strong evidence relating speed or density to the traffic values, so they are normalized to have equidistant average speed thresholds (0, 0.33, 0.66, 1) as done in a previous methodologies (Rybarczyk & Zalakeviciute, 2017; Rezzouqi et al., 2018). Then, a selected buffer is created around a 1500 m radius for each NO<sub>2</sub> station as NO<sub>2</sub> has been found to affect quality up to 1500 m downwind of major highways (Jerrett et al., 2007). The wind direction collected in the city meteorology station the same hour determines one of 8 cardinal directions, and calculates the average value of the traffic data within a 120 deg sector in the direction of the coming wind.

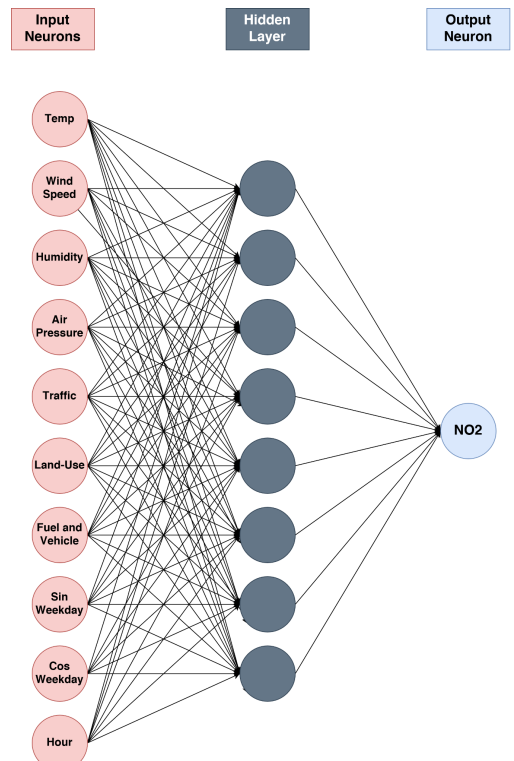
**Fuel and Vehicle Type:** The goal of using these datasets is to create a single value that represents how the amount of traffic correlates with the amount of emissions, and this is not accounted for in GMT. As different cities have different compositions of these vehicles, this data is an important aspect of comparing emissions between cities using traffic data. This value was determined by the variables concerning composition of gas vehicles per province and the composition of commercial vehicles including trailers per municipality. Both values were selected as both fuel and vehicle type are relevant factors, and they are averaged to create an arbitrary value representing emissions per amount of traffic. No suitable resource concerning the use of this data for weighting emissions was found, so the value was weighted as simply as possible. Adding more values with estimated weights is especially not useful with an ANN, which will learn the best weights for the model. These two values are combined into one for the goal of limiting model complexity, which assists in transferability.

**Land Use:** The Corine 2018 dataset was first reclassified into 11 more general land use RIO classes as used in Janssen et al.. Then, the 11 RIO classes were each weighted with optimized weight found in the study that relates each class with how it will affect the concentration of NO<sub>2</sub>. This study also found that a 2km buffer around each measurement site produced the best results, so this method was also used to calculate the average surrounding value.

### Model Development:

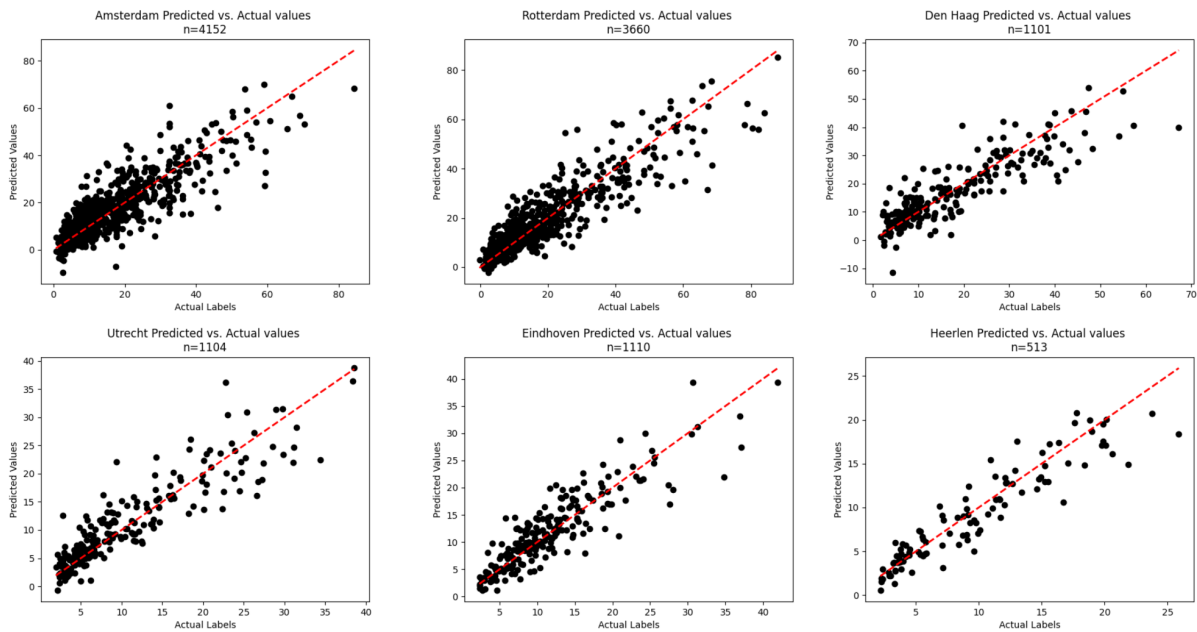
**Artificial Neural Network:** The algorithm used in this model is a Multi-Layer Perceptron Regressor. This is a type of Feed-Forward Neural Network that is commonly used in air pollution studies due to its simplicity and generalizability and has been found to be successful in studies of transferability (Alimisis et al., 2018; Zito et al., 2008). Figure 7 shows an example of a 10-input model with a single hidden layer of 8 neurons. While machine learning techniques and ANNs in particular are known for many forms of hyperparameterization, this methodology only attempts to optimize input variables and hidden layer size. Model structure is especially important for transferable models as more predictor values and hidden layers leads to more overtraining of the dataset, and less generalization (Molina-Cabello et al., 2019).

Figure 7: Example 10-8-1 ANN model



**Preliminary Model Validation:** Before the model is tested for transferability, its non-transferred performance for each city is validated so that a baseline of predictive accuracy for the study area and predictor variables can be established. A 10-100-50-1 architecture model was developed for each city and tested on unseen data. As seen in figure 8, a baseline capability was established with  $r^2$  ranging from 0.69-0.86.

Figure 8: Scatterplot results of 5FCV for each city



**Model Optimization:** While model optimization is not a part of the research goals of this study, creating a transferable model often involves a reduction in complexity by removing the amount of input neurons in the hidden layer and the total amount of predictor variables as well. A simple method of MLP feature extraction, known as Relative Importance (RI) was used. This methodology, first proposed by Garson, 1991, computes the weights between the layers of neurons, and then finds the relative importance of an input variable by the absolute value of the sum of its products divided by the sum of all products (Garson, 1991). The results of an RI calculation of all input variables for all collected training sets can be seen in table 1.

Table 1: Relative Importance (RI) for all training sets

Input Variable	RI (%)
Air Pressure:	22.632
Weekday:	10.154
Humidity:	9.13
Hour:	8.955
Temperature:	7.613
Fuel and Vehicle:	6.727
Wind Speed:	5.802
Land Use	3.985
Traffic Alternative:	2.569
Google Maps:	1.516

The RI values are calculated for each test, so that the best variables for the specific study area and model complexity are chosen. For the tests of this analysis, the top four RI variables for each calculation were used in the development of an optimised model. This is the base model to which GMT and the historical average traffic alternative are additionally added onto and tested. It should be noted that RI is a limited method of feature extraction as it only provides a linear relationship

between the input and output neuron (Garson, 1991). Many other more successful feature selection methodologies exist, but were determined out of the scope of this study.

**Evaluation:** The accuracy of each model is determined with both Mean Squared Error (MSE) and the Coefficient of Determination ( $r^2$ ). Lower MSE and higher  $r^2$  indicate a more accurate model. Both determinants utilize the relationship between observed and predictor values, but  $r^2$  is a representation of the variance of the data, while MSE assesses the average magnitude of errors. Some of the models in this study have negative  $r^2$  values as the models get less and less accurate. This may seem counter-intuitive for common understandings of  $r^2$  representing explained variance, but can actually come from evaluating models on different sets that they are fitted on if the predictions are bad enough (Kvålseth, 1985).

## Results

### Inter-Urban LOOCV:

For the first test of transferability, two inter-urban LOOCV tests were done for the cities of Amsterdam and Rotterdam. For every station, a training set was made of the other stations in the city and tested on that station's data. As Den Haag, Utrecht, and Eindhoven only had 3 measurement stations each, they were removed. An optimal model was found via using RI of the variables in a dataset of both Amsterdam and Rotterdam to inform trial-and-error feature selection. The optimal model for this evaluation was found to have 4 input variables: Air Pressure, Temperature, Fuel/Vehicle Type, Land-Use, with 20 hidden layers.

Table 2: Results of Inter-Urban LOOCV

Study Area	Model	MSE	$r^2$
Amsterdam stations = 12	OPT	85.02449	0.395478
	OPT + GMT	86.02358	0.38355
	OPT + ALT	114.9994	0.369143
Rotterdam stations = 10	OPT	74.77805	0.644899
	OPT + GMT	82.18628	0.646541
	OPT + ALT	76.84599	0.612211
Average	OPT	79.90127	0.5201885
	OPT + GMT	84.10493	0.5142245
	OPT + ALT	95.922695	0.490677

OPT = Optimal Variables (Air Pressure, Temperature, Fuel/Vehicle Type, Land-Use)

GMT = Google Maps Traffic

ALT = Alternate 2022 average traffic per hour

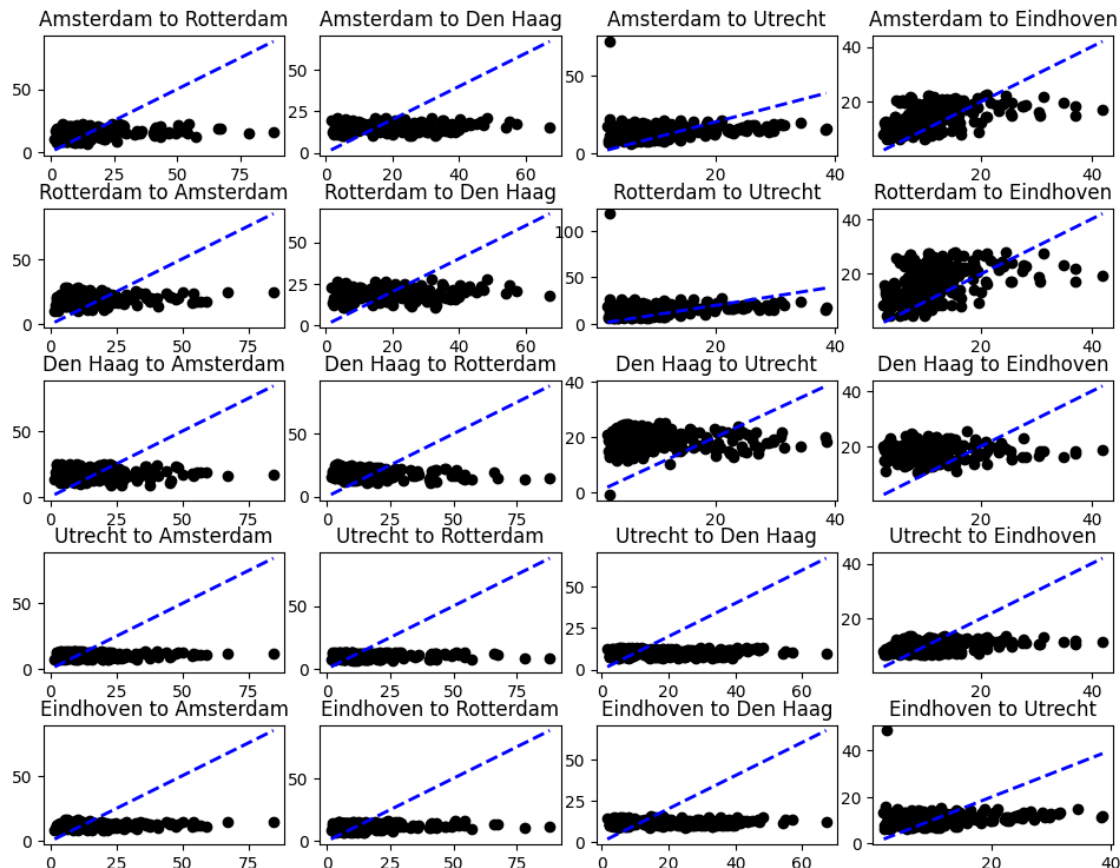
The Rotterdam LOOCV had higher average accuracy than the Amsterdam model mostly because of the poor prediction accuracy of a few Amsterdam stations. This may be due to the high concentration of NO<sub>2</sub> stations in the center of Amsterdam, with 3/4 of the stations within the A10 ring highway, the outside stations receive very different variations in NO<sub>2</sub> levels. The Rotterdam stations are comparatively much more evenly spaced and have similar surrounding

land-use. Because of this, Rotterdam may experience less general inter-city variation, which would improve LOOCV accuracy. In both cities, the optimized model performed the best, addition of GMT caused a slight decrease, while the alternative historical traffic was lower with higher variation between stations.

### Direct Transferability HV

Direct Intra-Urban transferability was tested for each of the five cities by creating a model for each city and testing its accuracy on the data from every other city. The optimal model was created by first finding the RI of the features in a dataset with all cities. The most important variables were found to be air pressure, weekday, hour of the day, and humidity with an 8 neuron hidden layer.

Figure 9: Scatterplots of Direct Intra-Urban Transfer Between All Cities (actual vs. predicted NO<sub>2</sub> concentration)



The scatter plots immediately show no predictive capability for the majority of the transferred models. Of the best performing model test (4 optimal variables) the only direct transfers with an  $r^2$  above zero were: Utrecht to Eindhoven ( $r^2=0.146$ ), Eindhoven to Utrecht ( $r^2=0.1$ ), and Amsterdam to Rotterdam ( $r^2=0.058$ ). A notable trend is that the models seem to do especially worse when they are shown a higher range of values than they were trained on. Cities like Eindhoven and Utrecht, whose measurements collect a maximum of 45, are more successfully transferred to.

Table 3: Results of Average Direct Intra-Urban Transfer for all Permutations

Data	Average MSE	Average $r^2$
OPT	149.7099	-0.16501
OPT + GMT	172.5462	-0.4408
OPT + ALT	172.9166	-0.48282

OPT = Optimal Variables (Air Pressure, Temperature, Fuel/Vehicle Type, Land-Use)

GMT = Google Maps Traffic

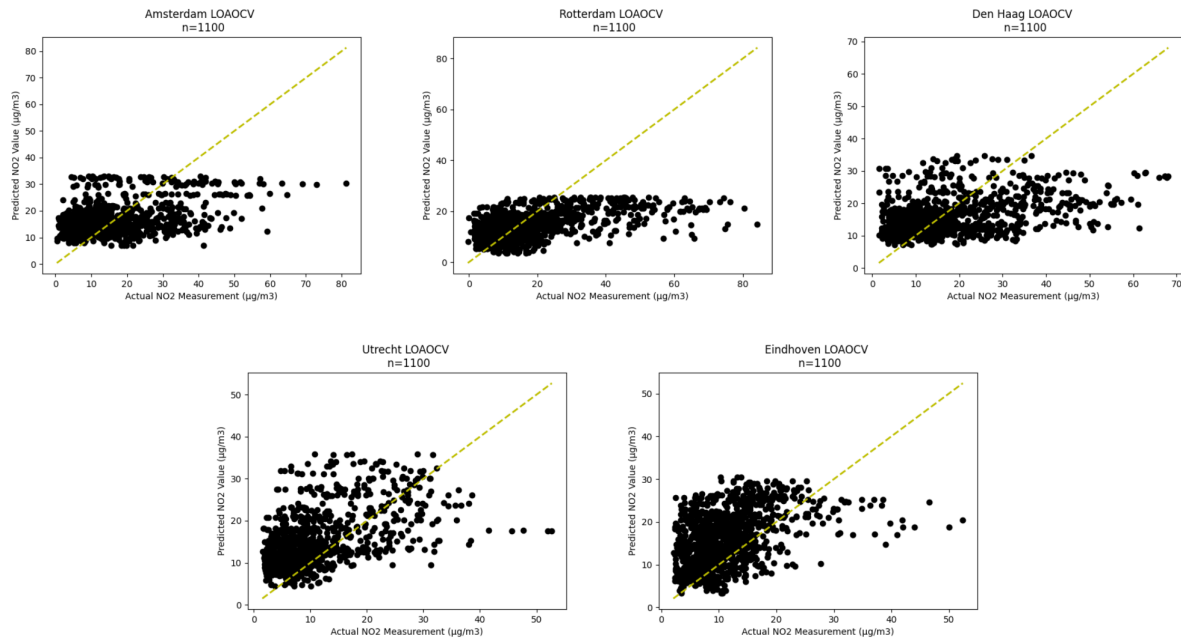
ALT = Alternate 2022 average traffic per hour

The results of the model comparison reveal that all models performed poorly, but GMT and the traffic alternative are more similar and perform much worse compared to the optimal than in the inter-urban LOOCV. Each model performed relatively similarly for each test of transferability and all had a similar standard deviation.

### Intra-Urban LOOCV

This intra-urban LOOCV was tested in the same manner as the inter-urban LOOCV, however the samples removed from the training set and tested are each city. The same optimal model as the direct transferability was found so it included 4 input variables: air pressure, weekday, hour of the day, and humidity with an 8 neuron hidden layer.

Figure 10: Scatterplot results of 5 city LOOCV



The best performing model was the optimized version, and three positive  $r^2$  measurements were found: (Rotterdam:  $r^2=0.196$ , Amsterdam:  $r^2=0.152$ , and Den Haag:  $r^2=0.151$ ). Noticably, much of the data is organized into identifiable horizontal lines, this is the result of having many repeated input variables. As each training set in the model is a station, many of the training sets share multiple values such as weather with the other training sets during the same hour. As many values were shared, not all predictor variables were independent as would be ideal, which likely caused the above effect. The training sets were created this way out of necessity as creating city-sized training sets significantly reduced the amount of data and

Table 4: Results of intra-urban LOOCV for each study area

made transferability impossible.

Study Area	Model	MSE	$r^2$
Amsterdam	OPT	122.409	0.152
	OPT + GMT	123.73	0.142
	OPT + ALT	130.175	0.098
Rotterdam	OPT	175.32	0.196
	OPT + GMT	175.833	0.193

	OPT + ALT	180.202	0.173
Den Haag	OPT	142.07	0.151
	OPT + GMT	141.338	0.155
	OPT + ALT	190.99	-0.14
Utrecht	OPT	70.368	-0.102
	OPT + GMT	73.6	-0.152
	OPT + ALT	60.16	0.0575
Eindhoven	OPT	72.594	-0.618
	OPT + GMT	77.388	-0.706
	OPT + ALT	76.243	-0.681
Average	OPT	116.5522	-0.0442
	OPT + GMT	118.3778	-0.0736
	OPT + ALT	127.554	-0.0985

OPT = Optimal Variables (Air Pressure, Temperature, Fuel/Vehicle Type, Land-Use)

GMT = Google Maps Traffic

ALT = Alternate 2022 average traffic per hour

### General Model Limit HV

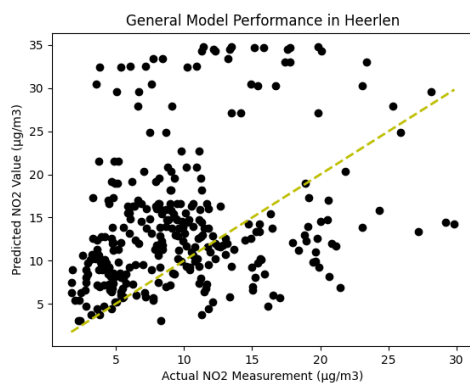
The final test of transferability is to test a general model, made of the five city data sets, on the smaller size city and surrounding area of Heerlen, in Limburg, NL. This model used the same architecture and input variables as the previous two.

Figure 11: Scatterplot results of General Model on Heerlen

Table 6: Results of General HV on Heerlen

Data	MSE	r <sup>2</sup>
OPT	87.307	-1.782
OPT + GMT	84.077	-1.679
OPT + ALT	90.985	-1.9

This test resulted in the lowest r<sup>2</sup> across all



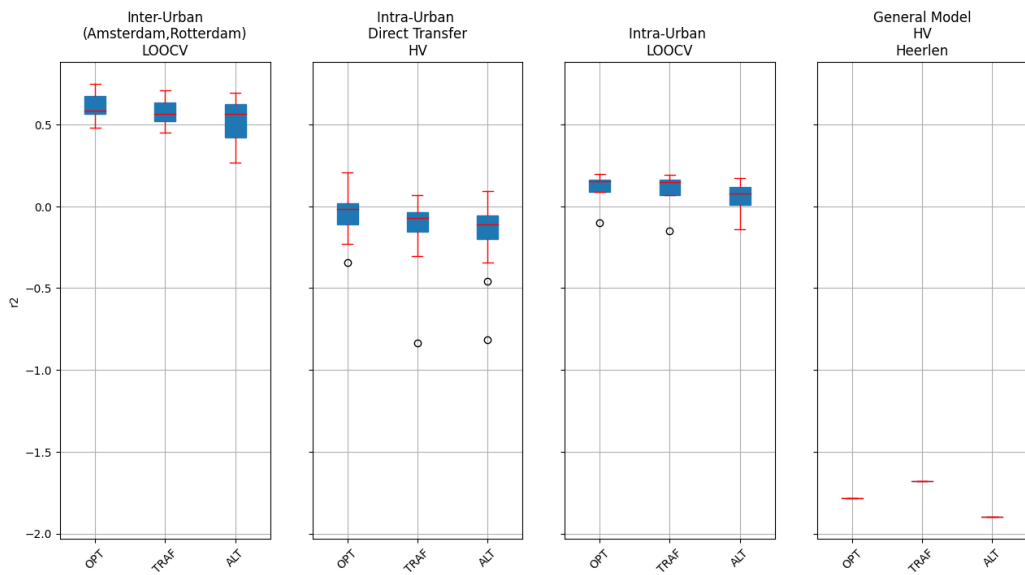
models. The model is seen to mostly over predict, but is still limited to the maximum tested values. This is the likely result of the low MSE with comparatively low r<sup>2</sup>. There are many small errors found from 0-15 µg, but large errors with more variable measurement occur above 15 µg.

GMT is the highest predicting model for this test, which is the only instance where it is not the optimized model.

### Aggregate Efficacy of GMT

Using the results from the three tests conducted on transferability, the scores of all three models are accumulated in figures 12 and 13 of  $r^2$  and MSE, respectively. By visual assessment of the box plots, the superiority of the optimized model is seen in almost every iteration. GMT is seen to have slightly worse predictions while the traffic alternative is worse than that. Significant inter-model variation is not seen from these results. This is especially the case in the intra-urban direct transfer as all models have similar standard deviations and do not vary much absolutely. Outliers are marked on the graphs by black circles and were found to occur both in the intra-urban HV and LOOCV.

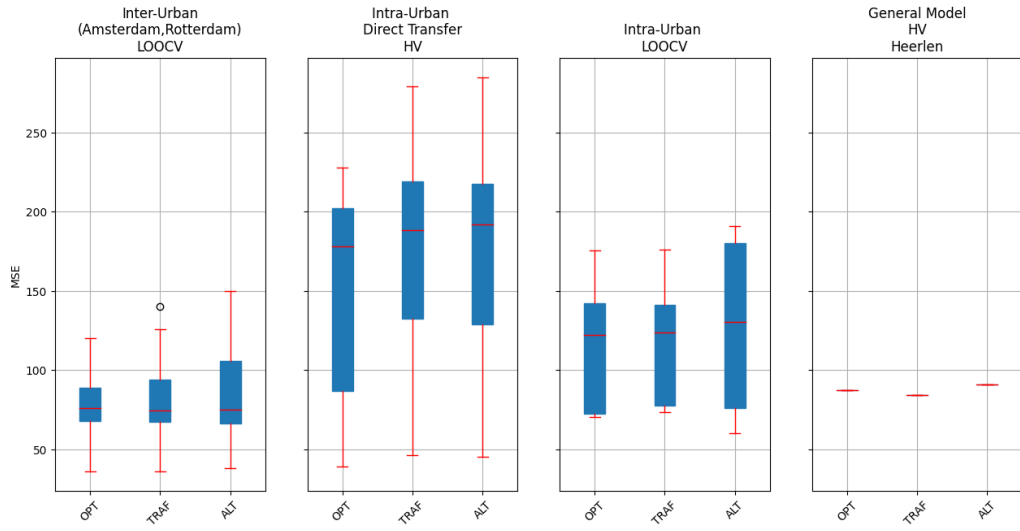
Figure 12: R<sup>2</sup> boxplot of all all test results for the three models



The same relations are generally repeated in both  $r^2$  and MSE boxplot. The most noticeable change to the plot is the lowered MSE in the general model test on Heerlen. While the MSE is

much lower and more comparable to the other models, the same trend of Google Maps with the lowest error replicated.

Figure 13: MSE boxplot of all test results for the three models



## Discussion

Comparison of model  $r^2$  is generally difficult as most studies have different study areas, scales of prediction, and number of sites (Wang et al., 2014). However, Rybarczyk and Zalakeviciute (2017) similarly utilized Google Traffic Data and collected measurements over the period of 2 months instead in Quito, Ecuador. The average prediction accuracy was  $r^2 = 0.64$ , while this study's similar individual city regression ranged from  $r^2 = 0.69-0.86$ . This study was able to utilize many more monitoring stations, which was likely a main source for the high accuracy results. This study also slightly underperformed in comparison to similar LOOCVs of FFNN LURs, with another methodologically comparable study finding  $r^2 = 0.72$  while the models tested in Amsterdam and Rotterdam had  $r^2 = 0.4$ , and  $0.64$  respectively(Li et al., 2021). Direct transferability (HV) between cities had some of the lowest reported accuracy where all

models had a negative average  $r^2$  value, and this is similarly reflected in the literature, with direct model transferability reported  $< 0.17$ , and 0.0001–0.349(Patton et al., 2015; Ma et al. 2020).

Intra-Urban LOOCV were among the most consistent results around  $r^2 = 0.2$ , but predicted poorly in comparison to a similar regional LOOCV in the Netherlands by Dijkema et al. (2011) with city-specific results of  $r=0.65$ . The general model test of Heerlen, to evaluate how the model could predict a very different location, the models performed the worst. This is in line with the expectations, especially due to the amount of data collected, and did not compare to the ESCAPE study European-wide  $r^2=0.56$  (Wang et al., 2014).

Unfortunately, there are several limitations to the proposed methods of this study. This study is mostly limited by the extent of its data collection. Data collection occurred real-time due to the inclusion of Google Maps which limited data collection to 2 months for this study.

Additional issues with KNMI API collection causing a bug in the program caused multiple days of data gaps throughout the period. As there was not enough data to create transferable models, any conclusions made are not relevant for the future of developing higher accuracy transferable models.

The leading motivation for this research was to explore solutions to the lack of low-cost measurement options in LMICS. Through the findings of the methodology, while the average accuracy was consistently the highest for the optimized models, addition of GMT had comparable results in most situations. So while Google Maps isn't shown to increase the transferability of models, as it provides similar average accuracy with an extra layer of complexity. Even though the models were scored on average to be the best, they are still limited to not having any information about the source of air pollution and are based mostly on the weather and time of day.

**Conclusion:**

This research identified a potential novel application of Google Maps for transferable air pollution prediction models. By collecting data within five of the largest cities in the Netherlands, optimized models were made for tests of transferability. To test the capability of GMT for these tests of transferability, models were developed with Google Maps and an alternative traffic predictor variable based on 2022 average traffic. The predictive accuracy of each test varied, but the relations between the models remained consistent with the optimized model the most accurate, then Google Maps closely, and then alternative. However, the variation between the specific models is not significant enough to not imply any strong benefits of Google Maps for Transferable Air Pollution models. While the conclusions that can be drawn are minimal, this study may still serve as preliminary research and provide a source of information for the possibility of using Google Maps as a data source in air pollution models. Along with additional data collection, more research should be conducted on the utilizing of GMT in general. The potential of this data source remains unchanged and further specification on its direct relation to on-ground vehicles should be found. Additionally, further investigation of the usefulness of GMT in LMIC transferable models should be done to see if the data source can actually be beneficial, as hypothesized.

**Works Cited:**

- Alimisis, A., Philippopoulos, K., Tzanis, C. G., & Deligiorgi, D. (2018). Spatial estimation of urban air pollution with the use of artificial neural network models. *Atmospheric Environment*, 191, 205–213. <https://doi.org/10.1016/j.atmosenv.2018.07.058>
- Allen, R. W., Amram, O., Wheeler, A. J., & Brauer, M. (2011). The transferability of NO and NO<sub>2</sub> land use regression models between cities and pollutants. *Atmospheric Environment*, 45(2), 369–378. <https://doi.org/10.1016/j.atmosenv.2010.10.002>
- Beelen, R., Hoek, G., Fischer, P., Brandt, P. A. van den, & Brunekreef, B. (2007). Estimated long-term outdoor air pollution concentrations in a cohort study. *Atmospheric Environment*, 41(7), 1343–1358. <https://doi.org/10.1016/j.atmosenv.2006.10.020>
- Berkowicz, R. (2000). OSPM - A Parameterise Street Pollution Model. *Environmental Monitoring and Assessment*, 65(1/2), 323–331. <https://doi.org/10.1023/a:1006448321977>
- Brauer, M., Hoek, G., van Vliet, P., Meliefste, K., Fischer, P., Gehring, U., Heinrich, J., Cyrys, J., Bellander, T., Lewne, M., & Brunekreef, B. (2003). Estimating Long-Term Average Particulate Air Pollution Concentrations: Application of Traffic Indicators and Geographic Information Systems. *Epidemiology*, 14(2), 228–239. <https://doi.org/10.1097/01.ede.0000041910.49046.9b>
- Briggs, D. J., de Hoogh, C., Gulliver, J., Wills, J., Elliott, P., Kingham, S., & Smallbone, K. (2000). A regression-based method for mapping traffic-related air pollution: application and testing in four contrasting urban environments. *Science of the Total Environment*, 253(1-3), 151–167. [https://doi.org/10.1016/s0048-9697\(00\)00429-0](https://doi.org/10.1016/s0048-9697(00)00429-0)

- Cabaneros, S. M., Calautit, J. K., & Hughes, B. R. (2019). A review of artificial neural network models for ambient air pollution prediction. *Environmental Modelling & Software, 119*, 285–304. <https://doi.org/10.1016/j.envsoft.2019.06.014>
- Caiza, L., Alvarez, R., Urquiza-Aguiar, L., Calderón-Hinojosa, X., & Ana Karina Zambrano. (2018). VTM. *Proceedings of the 15th ACM International Symposium on Performance Evaluation of Wireless Ad Hoc, Sensor, & Ubiquitous Networks.* <https://doi.org/10.1145/3243046.3243055>
- CBS. (2022a, May 16). *Verdeling personenauto's naar provincie, 2020-2021.* Centraal Bureau Voor de Statistiek.  
<https://www.cbs.nl/nl-nl/maatwerk/2022/20/verdeling-personenauto-s-naar-provincie-2020-2021>
- CBS. (2022b, November 23). *CBS Statline: Motorvoertuigen actief.* Opendata.cbs.nl.  
<https://opendata.cbs.nl/#/CBS/nl/dataset/85236NED/table?ts=1677346390720>
- Chen, J., de Hoogh, K., Gulliver, J., Hoffmann, B., Hertel, O., Ketzel, M., Bauwelinck, M., van Donkelaar, A., Hvidtfeldt, U. A., Katsouyanni, K., Janssen, N. A. H., Martin, R. V., Samoli, E., Schwartz, P. E., Stafoggia, M., Bellander, T., Strak, M., Wolf, K., Vienneau, D., & Vermeulen, R. (2019). A comparison of linear regression, regularization, and machine learning algorithms to develop Europe-wide spatial models of fine particles and nitrogen dioxide. *Environment International, 130*, 104934.  
<https://doi.org/10.1016/j.envint.2019.104934>
- Copernicus. (2018). *CLC 2018 — Copernicus Land Monitoring Service.* Copernicus.eu.  
<https://land.copernicus.eu/pan-european/corine-land-cover/clc2018?tab=download>

- Daly, A., & Zannetti, P. (2007). Air pollution modeling—An overview. *Ambient air pollution*, 15-28.
- Dijkema, M. B., Gehring, U., van Strien, R. T., van der Zee, S. C., Fischer, P., Hoek, G., & Brunekreef, B. (2011). A Comparison of Different Approaches to Estimate Small-Scale Spatial Variation in Outdoor NO<sub>2</sub> Concentrations. *Environmental Health Perspectives*, 119(5), 670–675. <https://doi.org/10.1289/ehp.0901818>
- Eskes, H., Boersma, F., Twan van Noije, Michel Van Roozendael, Isabelle De Smedt, Peters, U., & Meijer, E. W. (2008). Trends, seasonal variability and dominant NO<sub>x</sub> derived from a ten year record of NO<sub>2</sub> measured from space. *Journal of Geophysical Research*, 113(D4). <https://doi.org/10.1029/2007jd009021>
- European Environment Agency. (2021). *Netherlands - Air pollution country fact sheet* — European Environment Agency. [www.eea.europa.eu](http://www.eea.europa.eu).  
<https://www.eea.europa.eu/themes/air/country-fact-sheets/2021-country-fact-sheets/netherlands>
- Garson, G. (1991). *Interpreting neural-network connection weights*. 6(4), 46–51.  
<https://doi.org/10.5555/129449.129452>
- Google. (2023a). *Google Maps*. Google Maps; Google. <https://www.google.com/maps>
- Google. (2023b). *Google Maps Platform Coverage Details*. Google Developers.  
<https://developers.google.com/maps/coverage>
- Google Blog. (2009a, August 25). *Arterial traffic available on Google Maps*. Google Blog Maps.  
<https://maps.googleblog.com/2009/08/arterial-traffic-available-on-google.html>

Google Blog. (2009b, August 25). *The bright side of sitting in traffic: Crowdsourcing road congestion data*. Official Google Blog.

<https://googleblog.blogspot.com/2009/08/bright-side-of-sitting-in-traffic.html>

Hanna, R., Kreindler, G., & Olken, B. A. (2017). Citywide effects of high-occupancy vehicle restrictions: Evidence from “three-in-one” in Jakarta. *Science*, 357(6346), 89–93.

<https://doi.org/10.1126/science.aan2747>

Health Effects Institute. (2020). State of Global Air 2020. Special Report. In *State of Global Air*.  
<https://www.stateofglobalair.org/>

Hilpert, M., Johnson, M., Kioumourtzoglou, M.-A., Domingo-Relloso, A., Peters, A., Adria-Mora, B., Hernández, D., Ross, J., & Chillrud, S. N. (2019). A new approach for inferring traffic-related air pollution: Use of radar-calibrated crowd-sourced traffic data. *Environment International*, 127, 142–159. <https://doi.org/10.1016/j.envint.2019.03.026>

Hoek, G., Beelen, R., de Hoogh, K., Vienneau, D., Gulliver, J., Fischer, P., & Briggs, D. (2008). A review of land-use regression models to assess spatial variation of outdoor air pollution. *Atmospheric Environment*, 42(33), 7561–7578.

<https://doi.org/10.1016/j.atmosenv.2008.05.057>

Idrees, Z., & Zheng, L. (2020). Low cost air pollution monitoring systems: A review of protocols and enabling technologies. *Journal of Industrial Information Integration*, 17, 100123.  
<https://doi.org/10.1016/j.jii.2019.100123>

Janssen, S., Dumont, G., Fierens, F., & Mensink, C. (2008). Spatial interpolation of air pollution measurements using CORINE land cover data. *Atmospheric Environment*, 42(20), 4884–4903. <https://doi.org/10.1016/j.atmosenv.2008.02.043>

- Jerrett, M., Arain, A., Kanaroglou, P., Beckerman, B., Potoglou, D., Sahsuvaroglu, T., Morrison, J., & Giovis, C. (2005). A review and evaluation of intraurban air pollution exposure models. *Journal of Exposure Science & Environmental Epidemiology*, 15(2), 185–204. <https://doi.org/10.1038/sj.jea.7500388>
- Jerrett, M., Arain, M. A., Kanaroglou, P., Beckerman, B., Crouse, D., Gilbert, N. L., Brook, J. R., Finkelstein, N., & Finkelstein, M. M. (2007). Modeling the Intraurban Variability of Ambient Traffic Pollution in Toronto, Canada. *Journal of Toxicology and Environmental Health, Part A*, 70(3-4), 200–212. <https://doi.org/10.1080/15287390600883018>
- Karagulian, F., Belis, C. A., Dora, C. F. C., Prüss-Ustün, A. M., Bonjour, S., Adair-Rohani, H., & Amann, M. (2015). Contributions to cities' ambient particulate matter (PM): A systematic review of local source contributions at global level. *Atmospheric Environment*, 120, 475–483. <https://doi.org/10.1016/j.atmosenv.2015.08.087>
- KNMI. (2023). *KNMI Developor Portal*. [Developer.dataplatform.knmi.nl](https://developer.dataplatform.knmi.nl/). <https://developer.dataplatform.knmi.nl/get-started>
- Kvålseth, T. O. (1985). Cautionary Note aboutR2. *The American Statistician*, 39(4), 279–285. <https://doi.org/10.1080/00031305.1985.10479448>
- Li, Z., Ho, K.-F., Chuang, H.-C., & Yim, S. H. L. (2021). Development and intercity transferability of land-use regression models for predicting ambient PM10 PM2.5 NO2 and O3 concentrations in northern Taiwan. *Atmospheric Chemistry and Physics*, 21(6), 5063–5078. <https://doi.org/10.5194/acp-21-5063-2021>
- Luchtmeetnet. (2020, February). *Luchtmeetnet 2020 OpenAPI*. Luchtmeetnet 2020 OpenAPI. <https://api-docs.luchtmeetnet.nl/#948dfacc-f170-4815-8a07-bb256eae544d>

- Ma, X., Gao, J., Longley, I., Zou, B., Guo, B., Xu, X., & Salmond, J. (2022). Development of transferable neighborhood land use regression models for predicting intra-urban ambient nitrogen dioxide (NO<sub>2</sub>) spatial variations. *Environmental Science and Pollution Research*. <https://doi.org/10.1007/s11356-022-19141-x>
- Martin, R. V., Brauer, M., van Donkelaar, A., Shaddick, G., Narain, U., & Dey, S. (2019). No one knows which city has the highest concentration of fine particulate matter. *Atmospheric Environment: X*, 3, 100040. <https://doi.org/10.1016/j.aeaoa.2019.100040>
- Molina-Cabello, M. A., Passow, B. N., Dominguez, E., Elizondo, D., & Obszynska, J. (2019). Inferring Air Quality from Traffic Data Using Transferable Neural Network Models. *Advances in Computational Intelligence*, 15, 832–843.  
[https://doi.org/10.1007/978-3-030-20521-8\\_68](https://doi.org/10.1007/978-3-030-20521-8_68)
- Moon, J., Hong, J. G., & Park, T.-W. (2022). A Novel Method for Traffic Estimation and Air Quality Assessment in California. *Sustainability*, 14(15), 9169.  
<https://doi.org/10.3390/su14159169>
- Naiudomthum, S., Winijkul, E., & Sirisubtawee, S. (2022). Near Real-Time Spatial and Temporal Distribution of Traffic Emissions in Bangkok Using Google Maps Application Program Interface. *Atmosphere*, 13(11), 1803. <https://doi.org/10.3390/atmos13111803>
- OpenStreetMap Contributors. (2019). *OpenStreetMap*. OpenStreetMap.  
<https://www.openstreetmap.org>
- Patton, A. P., Zamore, W., Naumova, E. N., Levy, J. I., Brugge, D., & Durant, J. L. (2015). Transferability and Generalizability of Regression Models of Ultrafine Particles in Urban Neighborhoods in the Boston Area. *Environmental Science & Technology*, 49(10), 6051–6060. <https://doi.org/10.1021/es5061676>

- Poplawski, K., Gould, T., Setton, E., Allen, R., Su, J., Larson, T., Henderson, S., Brauer, M., Hystad, P., Lightowers, C., Keller, P., Cohen, M., Silva, C., & Buzzelli, M. (2008). Intercity transferability of land use regression models for estimating ambient concentrations of nitrogen dioxide. *Journal of Exposure Science & Environmental Epidemiology*, 19(1), 107–117. <https://doi.org/10.1038/jes.2008.15>
- Rezzouqi, H., Gryech, I., Sbihi, N., Ghogho, M., & Benbrahim, H. (2018). Analyzing the Accuracy of Historical Average for Urban Traffic Forecasting Using Google Maps. *Advances in Intelligent Systems and Computing*, 1145–1156. [https://doi.org/10.1007/978-3-030-01054-6\\_79](https://doi.org/10.1007/978-3-030-01054-6_79)
- RIVM. (2021, December 15). *The Netherlands almost meets EU air quality limit values in 2020 | RIVM*. [Www.rivm.nl](http://www.rivm.nl).
- <https://www.rivm.nl/en/news/netherlands-almost-meets-eu-air-quality-limit-values-in-2020>
- Russell, E. (2019). *9 things to know about Google's maps data: Beyond the Map | Google Cloud Blog*. Google Cloud Blog.
- <https://cloud.google.com/blog/products/maps-platform/9-things-know-about-googles-maps-data-beyond-map>
- Rybarczyk, Y., & Zalakeviciute, R. (2017). Regression Models to Predict Air Pollution from Affordable Data Collections. In *www.intechopen.com*. IntechOpen.
- <https://www.intechopen.com/chapters/57822>
- Selenium. (2023). *WebDriver*. Selenium. <https://www.selenium.dev/documentation/webdriver/>

- Sornsoongnern, P., Pueboobpaphan, S., & Pueboobpaphan, R. (2023). Innovative Dynamic Queue-Length Estimation Using Google Maps Color-Code Data. *Sustainability*, 15(4), 3466. <https://doi.org/10.3390/su15043466>
- Tang, U. W., & Wang, Z. S. (2007). Influences of urban forms on traffic-induced noise and air pollution: Results from a modelling system. *Environmental Modelling & Software*, 22(12), 1750–1764. <https://doi.org/10.1016/j.envsoft.2007.02.003>
- TomTom. (2023). *Amsterdam traffic report | TomTom Traffic Index*. Amsterdam Traffic Report | TomTom Traffic Index. <https://www.tomtom.com/traffic-index/amsterdam-traffic/>
- Wang, M., Beelen, R., Bellander, T., Birk, M., Cesaroni, G., Cirach, M., Cyrys, J., de Hoogh, K., Declercq, C., Dimakopoulou, K., Eeftens, M., Eriksen, K. T., Forastiere, F., Galassi, C., Grivas, G., Heinrich, J., Hoffmann, B., Ineichen, A., Korek, M., & Lanki, T. (2014). Performance of Multi-City Land Use Regression Models for Nitrogen Dioxide and Fine Particles. *Environmental Health Perspectives*, 122(8), 843–849. <https://doi.org/10.1289/ehp.1307271>
- WHO. (2016, May 12). *Air pollution levels rising in many of the world's poorest cities*. [Www.who.int.](http://www.who.int)  
[https://www.who.int/news/item/12-05-2016-air-pollution-levels-rising-in-many-of-the-w  
orld-s-poorest-cities](https://www.who.int/news/item/12-05-2016-air-pollution-levels-rising-in-many-of-the-world-s-poorest-cities)
- World Bank Group. (2021). *World Bank Climate Change Knowledge Portal*. [Climateknowledgeportal.worldbank.org.](https://climateknowledgeportal.worldbank.org)  
<https://climateknowledgeportal.worldbank.org/country/netherlands/climate-data-historica>
- Yegnanarayana, B. (2009). *Artificial neural networks*. PHI Learning Pvt. Ltd..

Zalakeviciute, R., Bastidas, M., Buenaño, A., & Rybarczyk, Y. (2020). A Traffic-Based Method to Predict and Map Urban Air Quality. *Applied Sciences*, 10(6), 2035.

<https://doi.org/10.3390/app10062035>

Zhang, X., Han, L., Wei, H., Tan, X., Zhou, W., Li, W., & Qian, Y. (2022). Linking urbanization and air quality together: A review and a perspective on the future sustainable urban development. *Journal of Cleaner Production*, 346, 130988.

<https://doi.org/10.1016/j.jclepro.2022.130988>

Zito, P., Chen, H., & Bell, M. C. (2008). Predicting Real-Time Roadside CO and NO<sub>2</sub> Concentrations Using Neural Networks. *IEEE Transactions on Intelligent Transportation Systems*, 9(3), 514–522. <https://doi.org/10.1109/TITS.2008.928259>

## Appendix:

### Appendix A: Data Table

<u>Input Data Source</u>	<u>Target Data Output</u>	<u>Occurrence / Date</u>	<u>Data Type</u>	<u>Resolution / Precision</u>	<u>Source</u>	<u>Quality</u>
Google Maps in Selenium Webdriver	Traffic Density IVs	Hourly from 6:00 - 19:00 2023/3/29 - 2023/5/29	png Screenshot	654x948 pixels	(Google, 2023)	<b>Acceptable.</b> Issues with Chromedriver and resolution output that caused gaps. Web scraping requires a lot of additional processing
OpenStreetMap road shape and type via QuickOSM (QGIS Plug-in)	Traffic Density IVs	2023	Vector Line Shapefile	Precision = 4 roads types: motorway, trunk, primary, secondary	(OpenStreetMap Contributors, 2019)	<b>Acceptable.</b> Very detailed, but requires additional processing to combine with Google Maps data
Meteorology Station API Request (Temperature, Wind Speed, Wind Direction, Relative Humidity, Air Pressure, Solar Radiance)	Meteorology IVs	Hourly from 6:00 - 19:00 2023/3/29 - 2023/5/29	Float values for each requested meteorological measurement in each city	Precision = (T=0.1 deg C; S=0.01 m/s; D=0.1 deg; H=1%; P=0.01 hPa; R=1 W m <sup>-2</sup> )	(KNMI, 2023)	<b>Poor.</b> Multiple empty values for prolonged times in all stations. Major impact on the amount of available training sets
Air Quality Station API request (NO <sub>2</sub> )	NO <sub>2</sub> Label DV	Hourly from 6:00 - 19:00 2023/3/29 - 2023/5/29	float values for each station in each city	Precision = 0.01 µg/m <sup>3</sup>	(Luchtmeetnet, 2020)	<b>High.</b> Few gaps in individual stations but not for long
Amount of Vehicles per Fuel Type per Province	Fuel Type IV	2020-2021	integers for each province	3 fuel types: electric, hybrid, and other. Precision = 1 Vehicle	(CBS 2022a)	<b>Good.</b> Recent sample. Could have more fuel types or high spatial resolution
Amount of Vehicles per Type per Municipality	Vehicle Type IV	2022/1/1	integers for each municipality	5 vehicle types: Commercial vehicles, trailers, motorcycles, mopeds, and other. Precision = 1 Vehicle	(CBS 2022b)	<b>High.</b> Recent sample. Specific to city / municipal level
Corine Land Cover (CLC)	Land-Use IV	2018	Raster	100m resolution	(Copernicus, 2018s)	<b>High.</b> Detailed enough resolution for city-scale spatial variance. Many land-use classifications.
Average 10km travel time for each hour in the day per city metro area	Traffic Alternative IV	2022	Min and sec	Precision: 10 sec	(TomTom, 2023)	<b>Good.</b> Specific to hour per day of the week. TomTom doesn't have the same volume of data collection as Google maps, but reportedly substantial.